HHS Public Access

Author manuscript

Nat Med. Author manuscript; available in PMC 2019 January 23.

Published in final edited form as:

Nat Med. 2018 September ; 24(9): 1384–1394. doi:10.1038/s41591-018-0125-4.

Metformin Inhibits Gluconeogenesis by a Redox-Dependent Mechanism *In Vivo*

Anila K. Madiraju[1,2,3,7], **Yang Qiu**[1,4,7], **Rachel J. Perry**[1], **Yasmeen Rahimi**[1], **Xian-Man Zhang**[1], **Dongyan Zhang**[1], **João-Paulo G. Camporez**[1], **Gary W. Cline**[1], **Gina M. Butrico**[1], **Bruce E. Kemp**[5], **Gregori Casals**[1], **Gregory R. Steinberg**[6], **Daniel F. Vatner**[1], **Kitt Falk Petersen**[1], and **Gerald I. Shulman**[1,2,3,*]

[1]Department of Medicine, Yale University School of Medicine, New Haven, CT, USA

[2]Department of Cellular & Molecular Physiology, Yale University School of Medicine, New Haven, CT, USA

[3]Howard Hughes Medical Institute, Yale University School of Medicine, New Haven, CT, USA

[4]Department of Endocrinology, Shengjing Hospital of China Medical University, Shenyang, China

[5]St. Vincent's Institute of Medical Research and Department of Medicine, University of Melbourne & Mary MacKillop Institute for Health Research, Australian Catholic University Fitzroy, VIC, 3065, Australia

[6]Departments of Medicine and Biochemistry and Biomedical Sciences, McMaster University, Hamilton, Ontario, Canada

Abstract

Metformin, the universal first-line treatment for type 2 diabetes, exerts its therapeutic glucose-lowering effects by inhibiting hepatic gluconeogenesis. However, the primary molecular mechanism of this biguanide remains unresolved, though it has been suggested to act, at least partially, by mitochondrial complex I inhibition. Here, we show that clinically-relevant plasma metformin concentrations achieved by acute intravenous, acute intraportal or chronic oral administration in awake normal and diabetic rats inhibit gluconeogenesis from lactate and glycerol but not from pyruvate and alanine, implicating an increased cytosolic redox state in mediating metformin's antihyperglycemic effect. All of these effects occurred independent of complex I

*Correspondence: gerald.shulman@yale.edu.

[7]Co-first author

Correspondence and requests for materials should be addressed to: gerald.shulman@yale.edu

Author Contributions

A.K.M., Y.Q., R.J.P., J.-P.C., D.F.V., K.F.P., G.I.S. designed the experimental protocols. A.K.M., Y.Q., Y.R., X-M.Z., D.Z., G.W.C., G.M.B., G.C., J.-P.G.C. K.F.P. performed the studies, A.K.M., Y.Q., R.J.P., X-M. Z., G.W.C., G.C., J.-P.G.C. analyzed the data, B.E.K. and G.R.S. supplied reagents, A.K.M., Y.Q., R.J.P, G.W.C., D.F.V., K.F.P., G.I.S. wrote the manuscript with contributions from all of the other authors.

The authors declare no competing financial interests.

Conflict of Interests

None of the authors have any conflicts of interest related to this study.

inhibition, evidenced by unaltered hepatic energy charge and citrate synthase flux. Normalizing the cytosolic redox state by infusion of methylene blue or substrates that contribute to gluconeogenesis independently of the cytosolic redox state abrogated metformin-mediated inhibition of gluconeogenesis *in vivo*. Additionally, in mice expressing constitutively active acetyl-CoA carboxylase, metformin acutely decreased hepatic glucose production and increased the hepatic cytosolic redox state without altering hepatic triglyceride content or gluconeogenic enzyme expression. These studies demonstrate that metformin, at clinically-relevant plasma concentrations, inhibits hepatic gluconeogenesis in a redox-dependent manner independent of reductions in citrate synthase flux, hepatic nucleotide concentrations, acetyl-CoA carboxylase activity, or gluconeogenic enzyme protein expression.

Keywords

Type 2 diabetes; metformin; redox physiology; redox shuttles; gluconeogenesis; liver metabolism; mitochondrial glycerophosphate dehydrogenase (GPD2); in vivo isotopic tracer labeling; Positional Isotopomer NMR Tracer Analysis (PINTA)

Introduction

It is well established that metformin will inhibit mitochondrial complex I activity, albeit at millimolar concentrations, and it has been generally postulated that its potent anti-diabetic effects occurs through this mechanism[1,2]. It has since been described that by diminishing electron transport chain activity, metformin decreases [ATP]:[ADP] and [ATP]:[AMP][1,2] and thus increases AMP kinase (AMPK) Thr[172] phosphorylation, promoting transcriptional down-regulation of gluconeogenic enzymes[3,4] and inhibition of acetyl-CoA carboxylase 1 (ACC1) and ACC2 activities[5]. Complex I inhibition and AMPK activation are possibly the most widely studied outcomes of metformin treatment, and they are invoked as the mechanism of metformin-mediated inhibition of hepatic lipogenesis, decrease in triglyceride accumulation, and increase in hepatic insulin sensitivity[6–10]. Additional studies have also hypothesized that metformin-mediated increases in AMP concentration can allosterically modulate key metabolic pathways to increase glycolytic flux over gluconeogenic flux[11], inhibit glucagon-mediated gluconeogenic gene transcription[12] or inhibit glucagon action via phosphodiesterase 4 (PDE4)[13]. Though compelling, these mechanisms are often delineated in the context of supra-pharmacological metformin dosing. They are also challenged by data showing that metformin, at clinically relevant plasma concentrations, does not appreciably alter energy charge or AMP concentration[14,15] and is capable of exerting its therapeutic effects in the absence of AMPK expression[11]. It is therefore plausible that there are critical actions of metformin independent of major alterations in adenine nucleotide concentration or AMPK action.

We previously demonstrated that metformin inhibits hepatic gluconeogenesis by decreasing mitochondrial glycerol-3-phosphate dehydrogenase (GPD2) activity[15]. This enzyme is a key component of the α-glycerophosphate shuttle, which is one of two shuttle systems required to transfer reducing equivalents from the cytosol to the mitochondria[16–18], altering cytosolic redox balance and suppressing hepatic gluconeogenesis[15]. In our previous work, we showed

that loss of hepatic GPD2 expression phenocopies metformin treatment. Furthermore, we demonstrated that metformin's ability to decrease plasma glucose concentrations and hepatic glucose production is abrogated when hepatic GPD2 protein expression is ablated genetically in GPD2 knockout mice or transiently in GPD2 antisense oligonucleotide treated rats[15]. In the present study, we use ^{13}C positional isotopomer tracer analyses to follow carbon flux *in vivo* to specifically ascertain that metformin, by inhibiting GPD2, targets hepatocellular redox metabolism to achieve its therapeutic effect in awake, unrestrained diabetic and non-diabetic rats.

Results

Redox regulation of gluconeogenesis varies with the carbon source. In particular, a more reduced cytosol (*i.e.*, increased cytosolic [NADH]:[NAD^+]) inhibits gluconeogenesis from lactate and glycerol[19,20] but not from alanine and pyruvate[21,22]. The key difference between these substrates is the increased sensitivity of lactate and glycerol to a reduced cytosol and thus increased cytosolic [NADH]:[NAD^+], since these substrates, unlike pyruvate or alanine, will themselves reduce the cytosol (Supplementary Fig. 1a). Glycerol, which can contribute to approximately 20–30% of hepatic gluconeogenesis under certain conditions[23,24], enters gluconeogenesis via the α-glycerophosphate shuttle and reduces the cytosol if processed by cytosolic glycerol-3-phosphate dehydrogenase (GPD1) (Supplementary Fig. 1b).

Of note, metformin decreased glucose production only from lactate and glycerol *in vitro,* reflecting the expected metabolic outcome of cytosolic redox-modulation as opposed to generalized inhibition of gluconeogenesis that may result from down-regulating the gluconeogenic transcriptional program[15]. Further evidence for a redox modulatory effect of metformin is provided by the observation that GPD2 inhibition by metformin increased liver cytosolic redox, reflected by a [lactate]:[pyruvate] > 10 that represses hepatic gluconeogenesis[20,25]. In isolated primary hepatocytes, metformin suppressed hepatic glucose production from gluconeogenic substrates that depend on cytosolic NADH (lactate and glycerol), but not from gluconeogenic substrates independent of cytosolic NADH [dihydroxyacetone (DHA), alanine, pyruvate] (Supplementary Fig. 1c). In contrast, the pyruvate carboxylase (PC) inhibitor phenylacetate and the cytosolic phosphoenolpyruvate carboxykinase (PEPCK-C) inhibitor 3-mercaptopicolinic acid both did not exhibit a substrate-selective pattern of inhibition. The substrate-specific effect observed with metformin treatment is a hallmark of a redox-mediated inhibition of gluconeogenesis and distinguishes this mechanism from all other proposed mechanisms for metformin inhibition of hepatic gluconeogenesis[2,3,5–13].

Impact of Acute Intravenous Metformin Injection on Substrate-Specific Contributions to Hepatic Gluconeogenesis in Normal and Rat Models of Type 2 Diabetes

To evaluate the importance of redox-modulation to the therapeutic effects of metformin *in vivo*, we measured the effect of acute intravenous (IV) metformin treatment on the specific contributions of lactate and alanine to gluconeogenesis in awake Sprague Dawley (SD) rats. We previously demonstrated that an acute IV dose of 50 mg kg^{-1} metformin can achieve plasma concentrations of 25 to 50 μM, approximating plasma concentrations observed in

individuals with type 2 diabetes (T2D) administered an acute oral dose (1 g) of metformin, and comparable to plasma concentrations seen in individuals with T2D being treated with chronic oral metformin dosing (1 g twice a day) (Supplementary Fig. 2)[26]. In contrast, prior studies in rats and mice have used very high parenterally administered doses ≥200 mg kg^{-1} of metformin[2,3,12,13,27–29] which elicit peak plasma concentrations of ~1,200 μM[15] that are supra-pharmacological. Doses that result in millimolar plasma metformin concentrations may have effects on hepatic metabolism (*e.g.*, complex I inhibition, etc.) that are not clinically relevant to the primary effects of metformin in individuals with T2D. Therefore, in order to achieve clinically relevant plasma metformin concentrations and avoid supra-pharmacological effects, all acute intravenous (IV) and intraportal vein studies were performed using 50 mg kg^{-1} metformin.

By using either [3-^{13}C]lactate or [3-^{13}C]alanine tracer, we were able to track ^{13}C carbons from both tracers which would be scrambled to the 1, 2, 5 and 6 carbon positions of glucose ([1-^{13}C], [2-^{13}C], [5-^{13}C], or [6-^{13}C]glucose) through hepatic gluconeogenesis. The fraction of total liver [1-^{13}C], [2-^{13}C], [5-^{13}C], and [6-^{13}C] glucose over total liver [3-^{13}C] substrate (lactate or alanine) provides the relative contribution of that substrate to gluconeogenesis. Entry of label from [3-^{13}C]lactate is influenced by redox state due to the cytosolic NADH-producing lactate dehydrogenase step (Fig. 1a), while [3-^{13}C]alanine labels glucose independent of cytosolic redox modulation (Fig. 1b). We observed that metformin acutely decreased plasma glucose concentrations in awake unrestrained 24h fasted, hepatic glycogen depleted, SD rats during both tracer infusion studies (Fig. 1c). This decrease was accompanied by a 3-fold higher liver [lactate]:[pyruvate] ratio, representative of an increase in the cytosolic redox state (Fig. 1d and Supplementary Fig. 3a,b), and a decrease in the hepatic mitochondrial redox state, represented by lower [β-hydroxybutyrate]:[acetoacetate] (Fig. 1e and Supplementary Fig. 3c,d). While acute IV metformin treatment suppressed endogenous glucose production (EGP) during both studies (Fig. 1f), the contribution of alanine to hepatic gluconeogenesis was unchanged, evidenced by the absence of any impact by metformin on the [1-^{13}C], [2-^{13}C], [5-^{13}C], [6-^{13}C] glucose / [3-^{13}C]alanine ratio compared to saline (denoted by a metformin/saline ratio of ~1). Metformin specifically decreased the contribution of lactate to hepatic glucose production, denoted by a ratio <1 for the [1-^{13}C], [2-^{13}C], [5-^{13}C], [6-^{13}C]glucose / [3-^{13}C]lactate fractions for metformin/saline (Fig. 1g and Supplementary Fig. 3e). This substrate-selective effect of metformin on lactate's contribution to glucose production, in these hepatic glycogen depleted rats, reveals that metformin modulates the redox state to inhibit hepatic gluconeogenesis *in vivo*. The observations that acute metformin treatment increased plasma glycerol and led to higher liver glycerol-3-phosphate (G-3-P) concentrations (Supplementary Fig. 3f,g) are consistent with metformin's potential mechanism of action to inhibit GPD2 activity, which in turn would decrease glycerol conversion to glucose. Metformin-induced reductions in plasma glucose concentration and inhibition of EGP were independent of changes in hepatic triglyceride and glycogen content (Supplementary Fig. 3h,i) indicating that the acute effect of metformin, under these conditions and at clinically relevant plasma concentrations, is to suppress hepatic gluconeogenesis[30,31] and is not mechanistically explained by increased hepatic fat oxidation[5,29] or by decreased net hepatic glycogenolysis[32,33]. Furthermore, expression of hepatic glucose-6-phosphatase (G6Pase) protein was unchanged, whereas

hepatic PEPCK-C and PC proteins were higher, while Ser133 phosphorylation of cAMP response element bind protein (CREB), the activated form of the key gluconeogenic transcriptional regulator, was higher (Supplementary Fig. 4a–d). These findings dissociate metformin's acute therapeutic effect from the transcriptional regulation of hepatic gluconeogenesis[3,12].

We found that hepatic AMPK was activated by acute metformin treatment, though surprisingly this did not translate to a detectable downstream effect on the AMPK substrate ACC, ACC phosphorylation by AMPK being a measure of AMPK activation (Supplementary Fig. 4e,f). Taken together these data demonstrate that metformin suppresses hepatic gluconeogenesis from glycerol and lactate but not from alanine *in vivo*, providing strong evidence that metformin inhibits gluconeogenesis by inhibition of GPD2 and modulation of the hepatic cytosolic and mitochondrial redox state.

In order to determine whether redox-mediated suppression of hepatic gluconeogenesis is a relevant mechanism of metformin action in diabetes, we also performed [3-^{13}C]lactate and [3-^{13}C]alanine tracer infusion studies in a well-established rodent model of T2D, the Zucker Diabetic Fatty (ZDF) rat. Fasting plasma glucose concentrations of these ZDF rats were markedly higher than those of SD rats, and acute metformin treatment induced a large reduction (>220 mg dL^{-1}) in plasma glucose concentrations (Fig. 2a). Hepatic cytosolic redox state was higher (Fig. 2b and Supplementary Fig. 5a,b) and mitochondrial redox state was lower with metformin treatment (Fig. 2c and Supplementary Fig. 5c,d) together with a greater than 50% lower rate of EGP in ZDF rats (Fig. 2d). As observed in SD rats, metformin did not impact alanine contributions to hepatic gluconeogenesis but specifically inhibited lactate contributions assessed by the metformin/saline ratio of the liver [1-^{13}C], [2-^{13}C], [5-^{13}C], [6-^{13}C]glucose to [3-^{13}C]lactate enrichments following infusion of [3-^{13}C]lactate (Fig. 2e and Supplementary Fig. 5e). Plasma glycerol and liver G-3-P concentrations were both increased (Supplementary Fig. 5f,g), again implicating inhibition of GPD2 as the target of acute metformin action decreasing hepatic gluconeogenesis in this rat model of poorly controlled T2D.

Metformin-mediated inhibition of EGP in the ZDF rats was also dissociated from changes in liver triglyceride or glycogen content (Supplementary Fig. 5h,i) and independent of alterations in the protein expression of key gluconeogenic enzymes (Supplementary Fig. 6a–d). Hepatic AMPK was activated, though again there was surprisingly no detectable change in the phosphorylation state of ACC (Supplementary Fig. 6e,f).

Effect of Acute IV Metformin on EGP and Lipid Metabolism in ACC DKI Mice

Considering the possibility that ACC phosphorylation is required for metformin's glucose-lowering effects[5], we examined the effect of acute metformin treatment in a mouse model with alanine knock-in mutations at Ser79 of ACC1 and Ser212 of ACC2 (ACC DKI mice) that has previously been described[5]. Acute IV metformin treatment decreased plasma glucose concentrations in both the ACC DKI mice and wild-type (WT) mice (Fig. 3a), increased hepatic cytosolic redox state and decreased the mitochondrial redox state (Fig. 3b,c). EGP was also significantly decreased in both ACC DKI and WT mice (Fig. 3d). The plasma glucose-lowering effect of metformin we observe in both WT and ACC DKI mice is

consistent with previous data showing that both chow and high fat diet (HFD) fed ACC DKI mice manifested a reduction in plasma glucose concentrations in response to a high dose of metformin [200 mg kg^{-1}, intraperitoneal (IP)][5]. Though the prior study reported that 50 mg kg^{-1} IP metformin did not impact blood glucose concentration in ACC DKI mice, basal EGP is a more sensitive indicator of metformin action, and this parameter was not measured in this prior study in response to acute metformin treatment[5].

As anticipated from data showing that metformin does not decrease hepatic triglyceride content in individuals with non-alcoholic fatty liver disease (NAFLD)[34–36] and does not impact fatty acid oxidation and lipid metabolism in individuals with T2D[37], we observed no effect on liver triglyceride content in either ACC DKI or WT mice with acute metformin, though liver triglycerides were elevated in ACC DKI mice compared to WT as previously reported[5] (Fig. 3e). Although activating phosphorylation of AMPK at Thr172 was increased, there was no effect on ACC phosphorylation in either WT or ACC DKI mice (Fig. 3f,g). Finally, while metformin treatment of both WT and ACC DKI mice lowered plasma glucose concentrations and EGP, it did not elicit changes in G6Pase, PC or PEPCK-C protein expression (Fig. 3h–j). These data demonstrate that metformin's ability to acutely suppress hepatic glucose production at clinically relevant plasma concentrations *in vivo* is not dependent on ACC activity or reductions in hepatic gluconeogenic enzyme expression.

Abrogation of Acute IV Metformin-Mediated Effects by Methylene Blue and Pyruvate/DHA Infusion in Normal SD Rats

Given that metformin treatment inhibits hepatic gluconeogenesis from redox-modulating substrates in normal SD and ZDF rats, we hypothesized that infusion of pyruvate and DHA would acutely abrogate the glucose lowering effects of metformin while infusion of lactate and glycerol would have no effect on metformin action in SD rats. Consistent with this hypothesis, infusion of pyruvate and DHA abolished metformin-induced reductions in plasma glucose concentrations but infusion of lactate and glycerol did not block metformin's glucose lowering effect (Fig. 4a). Concomitantly, the liver cytosolic redox state was lower with pyruvate and DHA infusion with no effect on the mitochondrial redox state (Fig. 4b,c). Hepatic G-3-P concentrations were maintained with pyruvate and DHA treatment, but were markedly elevated with infusion of lactate and glycerol (Fig. 4d). This is likely due to the impediment of excess glycerol substrate from entering gluconeogenesis due to inhibition of GPD2 by metformin. Finally, EGP was elevated in metformin-treated rats infused with pyruvate and DHA (Fig. 4e), but not in metformin-treated rats infused with lactate and glycerol. Taken together, these results confirm that metformin increases the cytosolic redox state and, in this manner, inhibits lactate and glycerol conversion to glucose, with no effect on pyruvate and DHA contributions to hepatic gluconeogenesis.

To further examine the modulation of redox state by metformin, we infused methylene blue intravenously into SD rats acutely treated with metformin. MB has been shown to influence cytosolic [NADH]:[NAD^+], reversing the effects of other agents that increase liver cytosolic redox state by decreasing [lactate]:[pyruvate] and [NADH]:[NAD^+][38]. Methylene blue administered 10 minutes following acute IV metformin infusion abrogated metformin's ability to lower fasting plasma glucose concentrations (Fig. 4f), alter liver cytoplasmic (Fig.

4g) and mitochondrial (Fig. 4h) redox ratios, and inhibit EGP (Fig. 4i). Taken together, these data demonstrate that by preventing metformin-mediated increases in the cytoplasmic redox state, methylene blue abrogated metformin's glucose-lowering effect. These findings offer further evidence that metformin inhibits hepatic gluconeogenesis by increasing the cytoplasmic redox state. While it has been suggested that the malate-aspartate shuttle should compensate for any reductions in the α-glycerophosphate shuttle activity[8,39,40], the increases in cytosolic redox state and decreases in mitochondrial redox state observed with both acute and chronic metformin treatment and with genetic knockdown of mitochondrial glycerol phosphate dehydrogenase[15] clearly show that this is not the case. Furthermore, the contribution to hepatic gluconeogenesis from glycerol, which is increased in individuals with T2D[41,42], is uniquely impacted by α-glycerophosphate shuttle inhibition. This effect of metformin would not be reversed by enhanced malate-aspartate shuttling.

Acute Intraportal Vein Infusion of Low Dose Metformin Decreases Plasma Glucose and Inhibits EGP by Modulating Hepatic Redox State

It has also been postulated that the acute glucose-lowering effects of metformin are primarily via gastrointestinal effects, and that direct effects on hepatic metabolism are seen with chronic treatment[27,43]. However, this hypothesis conflicts with studies in portal vein-strictured rats where orally-administered metformin had no effect on plasma glucose concentration[44]. Furthermore it was shown using [^{11}C]metformin tracer in humans that whether administered intravenously or orally, the drug is primarily taken up by the liver with low intestinal uptake[45]. Also challenging a primarily gastrointestinal effect is a study showing that metformin-stimulated GLP-1 secretion was insufficient to mediate metformin's acute glucose-lowering effect in individuals with T2D[46].

To provide further evidence that metformin's effect to inhibit hepatic gluconeogenesis is a direct effect on the liver and independent of effects in the gut or the gut microbiota, we performed portal vein metformin infusion studies. Acute infusion of 50 mg kg^{-1} metformin into the portal vein of normal SD rats gave rise to peak plasma metformin concentrations of ~130 μM, and hepatic metformin concentrations of ~25 μM two hrs following administration (Supplementary Fig. 7), comparable to the therapeutic range observed in individuals with T2D treated with metformin[47]. For these studies, we used a well-established rat model of T2D exhibiting both insulin resistance and partial β-cell failure: 4 week HFD-fed streptozotocin-nicotinamide (STZ) treated SD rats. Similar to systemic IV metformin treatment, acute portal vein 50 mg kg^{-1} metformin treatment in this rodent model of T2D acutely decreased plasma glucose concentrations within 30 minutes, and sustained this decrease in plasma glucose concentrations over 2 hrs (Fig. 5a). Portal vein metformin inhibited EGP by ~25% at 2 hrs (Fig. 5b). These data demonstrate that portal vein metformin infusion decreases plasma glucose and inhibits EGP, independent of gut metabolism. To determine whether portal vein metformin suppresses hepatic gluconeogenesis in a substrate-specific manner, we again infused [3-^{13}C]alanine or [3-^{13}C]lactate tracers in the HFD-STZ treated animals and measured the effect of portal vein metformin treatment on substrate turnover and clearance. While portal infusion of metformin did not affect alanine turnover or alanine clearance rates (Fig. 5c,d), lactate turnover and clearance were significantly lower with metformin treatment (Fig. 5e,f) as well

as β-hydroxybutyrate turnover (Fig. 5g). Finally, using [1,1,2,3,3-$^{2}H_5$]glycerol tracer, we determined that portal vein delivery of metformin led to significantly lower glycerol turnover and glycerol clearance (Fig. 5h,i). These redox-dependent substrate-specific effects of metformin on lactate and glycerol turnover and clearance rates were independent of changes in hepatic energy charge ([ATP]:[ADP] and [ATP]:[AMP]) (Supplementary Fig. 8a,b), AMPK activation and ACC phosphorylation (Supplementary Fig. 8c,d) and CREB phosphorylation (Supplementary Fig. 8e). The expression of hepatic PC protein remained unaltered, whereas expression of PEPCK-C protein was slightly increased (Supplementary Fig. 8f,g). Finally, using positional isotopomer NMR tracer analysis (PINTA) to non-invasively evaluate hepatic mitochondrial metabolism, we determined that portal vein metformin infusion inhibited flux through hepatic pyruvate carboxylase flux (V_{PC}) by approximately 30% (Fig. 5j). However, there was no impact on hepatic citrate synthase flux rates (V_{CS}; Fig. 5k), which would be predicted to decrease if metformin was causing significant inhibition of complex I activity.

Chronic Oral Metformin Treatment Decreases Plasma Glucose Concentration and Inhibits EGP in ZDF and HFD-STZ rat models of T2D Independent of Changes in Hepatic Nucleotide Concentrations, AMPK or ACC Phosphorylation or Gluconeogenic Enzyme Protein Expression

Though we were able to demonstrate that IV and intraportal delivery of metformin acutely decreased rates of hepatic gluconeogenesis by increasing the cytosolic redox state, we next wanted to examine whether this also occurred in a more clinically relevant context where metformin was administered orally in two well-established rat models of T2D. First, we treated ZDF rats with an upward titration of metformin dose, to mimic what is typically done in the clinic, in drinking water at 0.5 mg ml^{-1} for 7 days, 1.8 mg ml^{-1} for 7 days and finally 2.7 mg ml^{-1} for 14 days (final chronic dose 200–300 mg [kg-day] $^{-1}$). This upward oral metformin titration regimen led to clinically relevant plasma metformin concentrations of ~15 μM, and hepatic metformin concentrations of ~40 μM (Supplemental Fig. 9a,b) resulting in reductions in fasting plasma glucose concentrations of >100 mg dL^{-1} (Supplemental Fig. 9c). Neither liver citrate nor succinate concentrations were altered with metformin treatment, suggesting that complex I and complex II inhibition were not primarily responsible for metformin's therapeutic actions under these conditions (Supplemental Fig. 9d,e). However, similar to what was observed in the acute jugular and portal vein metformin infusion studies, chronic oral metformin treatment resulted in elevated hepatic G-3-P concentrations (Supplemental Fig. 9f). EGP was significantly inhibited by chronic oral metformin treatment (Supplemental Fig. 9g), and this effect was independent of changes in hepatic nucleotide concentrations (Supplemental Fig. 9h), AMPK or ACC phosphorylation (Supplemental Fig. 9i,j) and dissociated from changes in gluconeogenic enzyme protein expression (Supplemental Fig. 9k–n).

We then conducted a chronic, oral metformin treatment study in a second rat model of T2D, the STZ treated-HFD rats, and performed [3-^{13}C]lactate and [3-^{13}C]alanine tracer infusions to evaluate the effect of chronic metformin treatment on substrate-specific contributions to hepatic gluconeogenesis. HFD-STZ rats were treated with metformin in drinking water (3.5 mg ml^{-1}) over 14 days, achieving hepatic metformin concentrations of ~15 μM

(Supplemental Fig. 10a). Fasting plasma glucose concentrations were significantly lower with chronic oral metformin treatment in both [3-^{13}C]lactate and [3-^{13}C]alanine infused cohorts of HFD-STZ rats in the tracer infusion studies (Fig. 6a). Hepatic cytosolic redox state was increased with chronic oral metformin treatment as determined by an increased [lactate]:[pyruvate] (Fig. 6b and Supplemental Fig. 10b,c). Consistent with all of the other parenterally and orally administered metformin studies, hepatic G-3-P concentrations were increased with chronic oral metformin treatment (Fig. 6c) and EGP was inhibited by metformin in both tracer infusion cohorts (Fig. 6d).

Using PINTA, we were able to determine that pyruvate carboxylase flux (V_{PC}; Fig. 6e) was significantly decreased with chronic oral metformin treatment. However, consistent with the prior oral metformin treatment study, there was no impact on citrate synthase flux (V_{CS}; Fig. 6f) suggesting again that complex I inhibition is not the central mechanism of metformin action at clinically relevant liver metformin concentrations even in chronically treated diabetic rats. As observed in all of our other studies, we found that oral metformin treatment inhibited the contributions of [3-^{13}C]lactate to hepatic gluconeogenesis but had no effect on contributions of [3-^{13}C]alanine to gluconeogenesis in this diabetic rat model (Fig. 6g and Supplemental Fig. 10d). Metformin's impact on glycemia, hepatic gluconeogenesis and specific contributions of [3-^{13}C]lactate to gluconeogenesis were all independent of major changes in hepatic nucleotide concentrations (Supplemental Fig. 10e,f), both [ATP]:[ADP] and [ATP]:[AMP] being slightly increased in metformin treated rats. Phosphorylation of AMPK and ACC were not increased (Supplemental Fig. 11a,b) and though CREB phosphorylation was decreased, the protein expression levels of gluconeogenic enzymes (G6Pase, PC and PEPCK-C) were all unchanged (Supplemental Fig. 11c–f).

These data further support the hypothesis that redox modulation remains the relevant mechanism of metformin action in a context that better mimics the pharmacokinetics of metformin treated individuals with T2D.

Discussion

Several molecular mechanisms have been proposed for metformin's mode of action. Though metformin does inhibit complex I activity, this effect has only been observed at millimolar concentrations of the drug[1,2] and is therefore unlikely to be clinically relevant given that plasma concentrations in metformin treated individuals with T2D are typically in the 8–24 μM range[26,48], comparable to concentrations observed in this study. Furthermore, the ability of metformin to lower plasma glucose concentrations independently of the AMPK-ACC axis has been established, indicating that while AMPK activation and ACC inhibition may contribute to some of the beneficial effects of chronic metformin treatment[5], the fundamental mechanism by which metformin inhibits hepatic gluconeogenesis does not require AMPK activation and/or ACC1 and ACC2 inhibition. This is consistent with the inability of metformin to reverse NAFLD in individuals with T2D in the absence of weight loss[49,50] in contrast to the ability of ACC inhibitors to decrease hepatic steatosis in individuals with NAFLD[51].

An additional molecular target implicated in metformin action is adenylate cyclase, posited to be allosterically inhibited by increased [AMP] provoked by metformin. The resulting decrease in cAMP production would position metformin as an effective inhibitor of glucagon-stimulated hepatic gluconeogenesis. However, a recent study has demonstrated that metformin does not impact glucagon-stimulated gluconeogenesis in prediabetic individuals[52], suggesting that modulation of cAMP or cAMP-regulated gene expression does not explain metformin's therapeutic benefits in humans. The fact that modulation of cAMP-regulated gene expression is not essential to metformin action is also demonstrated by our previous studies[15], as well as our present findings showing no impact of acute or chronic metformin therapy on hepatic gluconeogenic enzyme protein expression in normal and T2D rats. Additionally, while acute metformin treatment in normal SD rats and both acute and chronic metformin treatment in two rat models of T2D inhibited hepatic gluconeogenesis, these therapeutic effects were not concomitant with AMPK activation, ACC phosphorylation, alterations in hepatic mitochondrial citrate synthase flux or altered liver triglyceride content. However, the redox state was consistently altered in tandem with any acute changes in plasma glucose and hepatic gluconeogenic rates in all three animal models, a phenomenon reaffirming what we saw in our previous metformin treatment studies[15]. These data suggest that previously described mechanisms of metformin action invoking complex I, AMPK-mediated ACC phosphorylation or decreased ectopic lipid accumulation in liver do not play a major role in the metformin's ability to acutely decrease hepatic gluconeogenesis at clinically relevant doses *in vivo*.

The redox-dependent, substrate-selective inhibition of gluconeogenesis observed *in vivo* with metformin treatment is consistent with the hypothesis that metformin inhibits GPD2 activity, either through direct and/or indirect mechanisms involving regulatory cofactors, increasing the hepatic cytosolic redox state and preventing lactate conversion to pyruvate and G-3-P conversion to DHAP. These substrate specific effects would not be predicted by metformin inhibition of hepatic mitochondrial complex I activity, charges in hepatic ATP/ADP/AMP concentrations, hepatic gluconeogenic transcriptional regulation, or AMPK activation. Metformin-induced increases in the hepatic cytosolic redox state has been demonstrated independently, both during acute intravenous and chronic oral metformin treatment increasing liver [lactate]:[pyruvate] and plasma lactate concentration without any effect on hepatic mitochondrial oxidative metabolism. Corroborating these data and the present findings are recent studies using hyperpolarized magnetic resonance spectroscopy demonstrating that 50 mg kg^{-1} IV metformin acutely increases cytosolic redox state in rat kidney, liver and heart[53,54]. Indeed, metformin-mediated increases in plasma lactate and the [lactate]:[pyruvate] ratio in humans have also been observed and underscore the clinical significance of a redox-based mechanism of action for metformin[55,56]. Numerous studies have established the importance of α-glycerophosphate shuttling in the modulation of gluconeogenic rates, showing that high protein and activity levels of hepatic GPD2 cause increased hepatic glucose production, and low hepatic GPD2 activity leads to diminished hepatic gluconeogenesis[57–59]. Our previous work revealed GPD2 as a key target of metformin action; however, the current *in vivo* carbon flux analysis demonstrates redox-modulation by metformin as a key element required to establish the physiological relevance of this mechanism of action. Here we show that metformin inhibits hepatic gluconeogenesis

in vivo, at clinically relevant plasma and liver concentrations, in a substrate-selective manner that is redox dependent and that would not be predicted by any other proposed mechanism[2,4–15]. This redox-dependent mechanism would also explain why metformin treatment is rarely associated with hypoglycemia given that gluconeogenesis will never be totally inhibited. Studying the impact of acute IV or intraportal infusion and chronic oral metformin treatment on carbon fluxes provided the added advantage of delineating the central, therapeutically relevant target of metformin action while minimizing potential supra-pharmacological effects of metformin (*e.g.*, complex I inhibition, complex II inhibition, complex IV inhibition, etc.)[1,2,11,60] that are not likely to be clinically relevant[48]. Taken together these studies demonstrate that metformin, at clinically relevant plasma concentrations, inhibits hepatic gluconeogenesis in a redox-dependent manner independent of reductions in citrate synthase flux, hepatic nucleotide concentrations, acetyl CoA carboxylase activity or hepatic gluconeogenic protein expression.

Online Methods

Hepatocyte Studies

Primary hepatocytes were isolated from 24-hour fasted Sprague-Dawley rats and treated with or without 100 μM metformin, 300 μM 3-mercaptopicolinic acid, or 4 mM phenylacetate in DMEM supplemented with 10 mM substrate (glycerol at 100 μM). Glucose was measured using Genzyme Glucose-SL reagent.

Human Metformin Pharmacokinetic Studies

The human metformin acute dosing pharmacokinetic study was reviewed and approved by the Yale Human Investigation Committee and written informed consent was obtained from each participant after explanation of the purpose, nature, and potential complications of the study. Study was performed according to the ethical guidelines and regulations as determined by the Yale Human Investigation Committee. Plasma metformin concentrations were measured every 10 min in three type 2 diabetic subjects following an oral 1 g dose of metformin, and in one type 2 diabetic subject on chronic metformin treatment (1g p.o. twice a day). Plasma metformin concentrations were measured by LC-MS/MS as previously described[2].

Animal Studies

Studies were performed in awake, unrestrained male rats. Male Sprague-Dawley and Zucker Diabetic Fatty rats were acquired from Charles River, and were administered regular chow and water ad libitum. Type 2 diabetes was induced in SD rats by feeding a safflower oil based high fat diet (Dyets, Inc. #112245) for four weeks, then treating rats with nicotinamide (80 mg kg^{-1}) and, 15 min later, low-dose streptozotocin (45 mg kg^{-1}), the Reaven rat model of T2D[61]. Rats with overnight fasted plasma glucose concentrations >300 mg dL^{-1} or plasma insulin <20 μU mL^{-1}, indicating severe insulinopenia (type 1 diabetic rodent model), were excluded from analysis. Rats were housed individually on a 12:12–hour light/dark cycle. Arterial lines were surgically implanted into the carotid artery and venous lines into the jugular vein of rats for the studies. A subset of rats underwent surgery to place catheters in the portal vein, carotid artery, and jugular vein. All animal studies included 5–12 rats per

group, aged 9–12 weeks and weighed 300–450 g at the time of study, except the portal vein studies where rats weighed 400–600 g. Animals were randomly allocated to treatment groups prior to collection of any data (e.g. weight) or surgical procedures and the studies were performed unblinded. Sample sizes were selected to detect moderate to large (>20%) differences. All studies were performed in awake, unrestrained animals. Acute metformin was administered intravenously (IV) in 0.9% saline at 50 mg kg^{-1} over 5 minutes, and via portal vein over 10 seconds. Unless otherwise stated, rats were fasted for 24 hours before studies were conducted. At the conclusion of all *in vivo* studies, rats were anesthetized by IV pentobarbital.

For chronic oral metformin treatment studies, rats were given *ad lib* access to drinking water with metformin, or untreated drinking water (control group). The drinking water metformin concentration was determined on a per-rat basis and adjusted twice-weekly, based on measured daily water intake and body weight. For ZDF rats, the metformin dose in the drinking water was uptitrated on a weekly basis until a glucose-lowering dose was found: the initial dose was 0.5 mg ml^{-1} for 1 week, this was increased to 1.8 mg ml^{-1} for 1 week, then 2.7 mg ml^{-1} for 2 weeks. ZDF rats were treated for a total of four weeks. For Sprague-Dawley streptozotocin-high fat diet fed rats, metformin treatment was at 3.5 mg ml^{-1} throughout a 2 week study.

In the acute IV metformin studies in SD and ZDF rats, contributions of lactate and alanine to hepatic gluconeogenesis were measured by continuous [3-^{3}H]glucose tracer infusion at 0.1 μCi min^{-1} and [3-^{13}C]lactate or [3-^{13}C]alanine at 40 μmol kg^{-1} min^{-1} for 120 minutes following a 5 min 120 μmol kg^{-1} min^{-1} prime. In the chronic oral metformin study in HFD-STZ rats, substrate contribution to hepatic gluconeogenesis was measured by continuous [^{3}H] glucose tracer infusion at 0.1 μCi min^{-1} and [3-^{13}C]lactate or [3-^{13}C]alanine at 10 μmol kg^{-1} min^{-1} for 120 minutes following a 5 min 30 μmol kg^{-1} min^{-1} prime. Positional isotopomer NMR tracer analysis (PINTA) was used to non-invasively evaluate hepatic mitochondrial metabolism.[62] Label in hepatic lactate, alanine and glucose was assessed by nuclear magnetic resonance (NMR) spectroscopy and GC/MS as previously described[63]. Briefly, ~4–6 g ground liver samples were extracted for NMR in ~30 mL 7% perchloric acid. The pH of the supernatant was adjusted to 6.5–7.5 using 30% potassium hydroxide and lyophilized. Extract was resuspended in 800 μL potassium phosphate buffer: 2.4 mM NaCOOH, 30 mM K_2HPO_4, 10 mM KH_2PO_4 and 20 mM DMSO in 100% D_2O. 13C NMR spectra were collected using the AVANCE 14 500-MHz NMR spectrometer (Bruker Instruments). Total glucose enrichment in the NMR extracts was determined by treating with methanol, drying overnight and derivitizing with 1:1 acetic anhydride:pyridine. The total [1-^{13}C], [2-^{13}C], [5-^{13}C], and [6-^{13}C] enrichment were measured by GC/MS. The ^{13}C NMR spectra were used to determine relative positional enrichments of [^{13}C] glucose[62]. Enrichment of the 2 and 3 positions of alanine or lactate from [3-^{13}C]lactate or alanine tracer was measured by proton-observed, carbon-edited (POCE) NMR[64].

For the lactate and β-OHB turnover studies using the type 2 diabetes rat model (HFD fed, partial β-cell ablation), rats underwent a primed-continuous arterial infusion with [3-^{13}C]lactate (Sigma), [1,2,3,4,5,6,6-$^{2}H_7$]glucose, and [$^{13}C_4$]sodium β-hydroxybutyrate. Prime was 3x the continuous rates for 5 minutes, followed by continuous tracer infusion at

10 μmol kg^{-1} min^{-1} [3-^{13}C]lactate, 0.1 mg kg^{-1} min^{-1} [1,2,3,4,5,6,6-$^{2}H_7$]glucose, and 0.1 mg kg^{-1} min^{-1} [$^{13}C_4$]sodium β-hydroxybutyrate for 120 minutes. For alanine and glycerol turnover, rats were primed for five minutes at 3x the continuous rates and then continuously infused for 120 minutes with tracer as follows: 10 μmol kg^{-1} min^{-1} [3-^{13}C]alanine, 0.1 μCi min^{-1} [3-^{3}H]glucose, and 0.1 mg kg^{-1} min^{-1} [1,1,2,3,3 $^{2}H_5$]glycerol. Rats were infused at this rate for another 120 minutes after acute portal vein infusion of 50 mg kg^{-1} metformin to measure metformin-mediated alteration of turnover rates. Blood was sampled at 2 hours and 4 hours, and tissues were acquired by rapid freeze-clamp within 10 seconds of euthanizing the animals.

β-OHB and glycerol turnover were measured as we have described[65]. Lactate turnover was measured by GC/MS using the same derivatization protocol as was employed to measure β-OHB enrichment. Plasma β-OHB and lactate concentrations were measured by COBAS, and plasma glycerol by GC/MS. Clearance of each substrate was calculated as the ratio of the turnover rate divided by the plasma concentration.

EGP during the substrate infusion and MB studies was measured using continuous 1 mg kg^{-1} min^{-1} arterial infusion of [6,6-$^{2}H_2$]glucose following a 5 min 3 mg kg^{-1} min^{-1} prime. Rats were treated with an acute 2 mg kg^{-1} IV bolus of MB within the first 5 min of the study. Pyruvate or lactate was infused at 20 μmol kg^{-1} min^{-1}, and DHA or glycerol was infused at 10 μmol kg^{-1} min^{-1} throughout the course of the study (120 min). Plasma glucose was measured on the YSI 2700 Biochemistry Analyzer from sampled venous blood.

Whole-body ACC1/2 double knock-in mice were a kind gift from Dr. Gregory R. Steinberg, McMaster University and Bruce Kemp, University of Melbourne. Whole-body ACC1/2 double knock-in mice were generated by Ozgene (Perth Australia)[5]. Catheters were surgically implanted into the jugular vein of mice 5–7 days prior to performing glucose infusion studies as previously described[66]. Mice were fasted overnight prior to the studies, and infused with [3-^{3}H]glucose at a rate of 0.05 μCi min^{-1} for 120 minutes to measure basal glucose turnover. Mice were then given acute metformin (50 mg kg^{-1}, IV) with continued [3-^{3}H]glucose infusion for another 120 minutes to measure metformin's effects on glucose turnover. Mice were restrained during the studies. Tissues were rapidly acquired and freeze-clamped within 10 seconds of euthanizing the animals.

All studies involving animals were conducted with prior approval from Yale University Institutional Animal Care and Use Committee (IACUC) in compliance with the ethical standards outlined by the IACUC.

Metabolite Measurement

Plasma glucose was measured on the YSI 2700 Biochemistry Analyzer. Surrogate metabolites for redox ratios were measured using enzymatic methods and by measuring NADH absorbance at 340 nm. Spectrophotometric measurements were made using the Flexstation 3 Benchtop Multi-Mode Microplate Reader (Molecular Devices). Liver metabolites were measured from PCA-extracted samples immediately after collection. Plasma glycerol was measured from de-proteinized plasma samples derivitized with acetic anhydride and pyridine. Glycerol was measured by GC/MS using an added internal standard,

[2-^{13}C]glycerol. Hepatic glycogen content was assessed by amyloglucosidase digestion as previously described[67]. Liver triglycerides were measured as previously described[68]. Liver lactate was measured from samples extracted by methanol:water (1:1 vol:vol ratio) on the YSI 2700 Biochemistry Analyzer. Hepatic G-3-P was measured by LC/MS/MS. Liver glycogen was measured by hydrolysis of glycogen and measure of glucose on the YSI 2700 Biochemistry Analyzer.

GC-MS Analysis of Pyruvate

For measurement of liver pyruvate, liver samples (100–150 mg) were homogenized together with 4% *o*-phenylene-diamine in 4N HCl solution, 16% sulfosalicilic acid (at a 1:1 vol:vol ratio) and α-ketoglutaric acid-d3 (internal standard). After centrifugation, the supernatant was heated for 45 min at 90°C to complete *o*-phenylene-diamine derivatization. After cooling, the samples were extracted twice with ethyl acetate, dried under nitrogen and further derivatized with BSTFA + 1% TMCS and pyridine (v 1:1, 30 min at 45°C then overnight at room temperature). Samples were analyzed by GC/MS (Agilent G1530A-5975C) in CI mode using isobutane as the reagent gas, and was equipped with an HP-1 capillary column (25m x 0.2mm ID, 0.33μm film thickness). The column temperature was initially held at 150°C for 1 minute, then ramped up 15°C min^{-1} to 220°C for a final hold time of 3 minutes. Data was recorded in selected ion monitoring (SIM) mode for pyruvate ions *m/z* 233–237 (Rt=4.0 min) and α-ketoglutaric acid-d3 ion *m/z* 278 (Rt=5.1 min).

LC-MS/MS Quantitation of Citrate and Succinate

Frozen tissue (~100 mg) was weighed in a 2.0 mL microcentrifuge tube, and then added 1.5 mL of pre-chilled methanol/water (50:50, v/v) solution containing 0.1 μmol of the internal standards (citric acid-$^{13}C_6$ and succinic acid-$^{13}C_4$), followed by disruption at 30 Hz for 2.0 min (Qiagen Tissue Lyser) and centrifugation (4000 rpm) at 4°C for 10 min. The supernatant was filtered with a nanosep 100K centrifugal device (Pall Life Science) before LC-MS/MS analysis. LC-MS/MS analysis was performed on an Applied Biosystems 6500 QTRAP (Foster City, CA), equipped with a Shimadzu ultrafast liquid chromatography (UFLC) system. Electrospray ionization (ESI) with a negative mode was used, and the ion-pair dependent parameters were optimized. The optimized parameters: curtain gas (14), collision gas (medium), ionization potential (−4500 V), probe temperature (500 ^{0}C), ion source gas 1 (60), ion source gas 2 (60) and EP (10 V). The ion-pair dependent parameters, CE: −10 ~ −30 V; DP : −20 ~ −60; CXP: −5 ~ −20 V. A Thermo Hypercarb HPLC column (100 mm x 3 mm) was used with a mixed solvent of 10 mM ammonium acetate solution and acetonitrile. Metabolites were monitored with MRM mode together with their C^{13} labeled internal standards (citric acid-$^{13}C_6$ and succinic acid-$^{13}C_4$). Citrate and citrate-$^{13}C_6$ were measured with ion pairs of 191/173 and 197/179 respectively; and succinate and succinate-$^{13}C_4$ were measured with ion pairs of 117/99 and 121/103, respectively. Metabolite concentrations were calculated from peak area ratios of the metabolites with their internal standards.

Western Blotting

Liver lysates were made by homogenizing pulverized, freeze-clamped liver tissue in lysis buffer (50 mM Tris-HCl pH 7.4, 1 mM EGTA, 150 mM NaCl, 5 mM $MgCl_2$, 1% NP-40) with added cOmplete protease inhibitor tablet (Roche) per 50 mL buffer. SDS samples were prepared by adding 2x SDS sample buffer (20% glycerol, 120 mM Tris-HCl pH 6.8, 4% SDS, 0.02% bromophenol blue, 4% β-mercaptoethanol) to one volume of lysate and boiling at 95°C for 5 min. Samples were run on Novex 4–12% Tris-Glycine gels (Invitrogen) and gels were transferred to PVDF membranes by semi-dry transfer. Antibodies used to determine protein expression were: PEPCK-C H-300 (Santa Cruz Biotechnology, Cat. No.: sc-32879), PCB H-2 (Santa Cruz Biotechnology, Cat. No.: sc-271493), Phospho-CREB Ser133 87G3 (Cell Signaling, Cat. No.: 9198), CREB 48H2 (Cell Signaling, Cat. No.: 9197), Phospho-AMPKα Thr172 40H9 (Cell Signaling, Cat. No.: 2535), AMPKα (Cell Signaling, Cat. No.: 2532), GAPDH D16H11 XP® (Cell Signaling, Cat. No.: 5174), G6Pase (Santa Cruz Biotechnology, Cat. No.: sc-27198), Phospho-ACC (Cell Signaling, Cat. No.: 3661), and ACC (Cell Signaling, Cat. No.: 3676)

Statistical analysis

All data are expressed as mean ± SEM except for the metformin/saline substrate contribution data, which is graphed as mean ± SD. *P* values less than 0.05 were considered statistically significant differences as determined by unpaired two-tailed Student's *t* test or ANOVA. For the metformin/saline ratios, effects size was calculated using Cohen's standard *d* and deemed a significant effect size if the value was greater than 0.6. Data shown are representative of repeated experiments performed as indicated; where not indicated, a single experiment was performed. All replicates are biological replicates unless otherwise indicated.

Data Availability

The datasets generated during and/or analyzed during the current study are available from the corresponding author on reasonable request.

Supplementary Material

Refer to Web version on PubMed Central for supplementary material.

Acknowledgments

The authors would like to thank Jianying Dong, Mario Kahn, Sylvie Dufour, John Stack, Yanna Kosover, Ali Nasiri, Xiaoxian Ma, Wanling Zhu, and Kathy Harry for their technical support and Drs. Varman Samuel, Sonia Caprio and Dick Kibbey for helpful discussions. This publication was supported by grants from the U.S. Department of Health and Human Services: R01 DK113984, P30 DK45735, P30 DK034989, K99 CA215315 and R01 DK114793. Its contents are solely the responsibility of the authors and do not necessarily represent the official view of NCRR or the NIH. Gregory R. Steinberg is supported by grants and fellowships from a Canada Research Chair in Metabolism and Obesity, the J. Bruce Duncan Endowed Chair in Metabolic Diseases at McMaster University and Diabetes Canada. BEK is supported by grants and a Fellowship (BEK) from the National Health and Medical Research Council (1068813 and 1085460) and the Victorian Government Operational Infrastructure Support Scheme.

References

1. Owen MR, DE, Halestrap AP. Evidence that metformin exerts its anti-diabetic effects through inhibition of complex 1 of the mitochondrial respiratory chain. Biochem J. 2000; 348(Pt 3):607–614. [PubMed: 10839993]
2. El-Mir M-Y, NV, Fontaine E, Averet N, Rigoulet M, Leverve X. Dimethylbiguanide Inhibits Cell Respiration via an Indirect Effect Targeted on the Respiratory Chain Complex I. J Biol Chem. 2000; 275:223–228. [PubMed: 10617608]
3. He L, SA, Djedjos S, Miller R, Sun X, Hussain MA, Radovick S, Wondisford FE. Metformin and insulin suppress hepatic gluconeogenesis through phosphorylation of CREB binding protein. Cell. 2009; 137:635–646. [PubMed: 19450513]
4. Cao J, MS, Chang E, Beckwith-Fickas K, Xiong L, Cole RN, Radovick S, Wondisford FE, He L. Low concentrations of metformin suppress glucose production in hepatocytes through AMP-activated protein kinase (AMPK). J Biol Chem. 2014; 289:20435–20446. [PubMed: 24928508]
5. Fullerton MD, GS, Marcinko K, Sikkema S, Pulinilkunnil T, Chen ZP, O'Neill HM, Ford RJ, Palanivel R, O'Brien M, Hardie DG, Macaulay SL, Schertzer JD, Dyck JR, van Denderen BJ, Kemp BE, Steinberg GR. Single phosphorylation sites in Acc1 and Acc2 regulate lipid homeostasis and the insulin-sensitizing effects of metformin. Nat Med. 2013; 19:1649–1654. [PubMed: 24185692]
6. Cool B, et al. Identification and characterization of a small molecule AMPK activator that treats key components of type 2 diabetes and the metabolic syndrome. Cell Metab. 2006; 3:403–416. [PubMed: 16753576]
7. Guigas B, VB. Targeting AMPK: From Ancient Drugs to New Small-Molecule Activators. EXS. 2016; 107:327–350. [PubMed: 27812986]
8. Rena G, HD, Pearson ER. The mechanisms of action of metformin. Diabetologia. 2017; 60:1577–1585. [PubMed: 28776086]
9. Shaw RJ, LK, Vasquez D, Koo SH, Bardeesy N, Depinho RA, Montminy M, Cantley LC. The kinase LKB1 mediates glucose homeostasis in liver and therapeutic effects of metformin. Science. 2005; 310:1642–1646. [PubMed: 16308421]
10. Smith BK, MK, Desjardins EM, Lally JS, Ford RJ, Steinberg GR. Treatment of nonalcoholic fatty liver disease: role of AMPK. Am J Physiol Endocrinol Metab. 2016; 311:E730–E740. [PubMed: 27577854]
11. Foretz M, HS, Leclerc J, Zarrinpashneh E, Soty M, Mithieux G, Sakamoto K, Andreelli F, Viollet B. Metformin inhibits hepatic gluconeogenesis in mice independently of the LKB1/AMPK pathway via a decrease in hepatic energy state. J Clin Invest. 2010; 120:2355–2369. [PubMed: 20577053]
12. Miller RACQ, Xie J, Foretz M, Viollet B, Birnbaum MJ. Biguanides suppress hepatic glucagon signalling by decreasing production of cyclic AMP. Nature. 2013; 494:256–260. [PubMed: 23292513]
13. Johanns M, LY, Hsu MF, Jacobs R, Vertommen D, Van Sande J, Dumont JE, Woods A, Carling D, Hue L, Viollet B, Foretz M, Rider MH. AMPK antagonizes hepatic glucagon-stimulated cyclic AMP signalling via phosphorylation-induced activation of cyclic nucleotide phosphodiesterase 4B. Nat Commun. 2016; 7:10856. [PubMed: 26952277]
14. Hawley SA, GA, Olsen GS, Hardie DG. The antidiabetic drug metformin activates the AMP-activated protein kinase cascade via an adenine nucleotide-independent mechanism. Diabetes. 2002; 51:2420–2425. [PubMed: 12145153]
15. Madiraju AK, ED, Rahimi Y, Zhang XM, Braddock DT, Albright RA, Prigaro BJ, Wood JL, Bhanot S, MacDonald MJ, Jurczak MJ, Camporez JP, Lee HY, Cline GW, Samuel VT, Kibbey RG, Shulman GI. Metformin suppresses gluconeogenesis by inhibiting mitochondrial glycerophosphate dehydrogenase. Nature. 2014; 510:542–546. [PubMed: 24847880]
16. Cederbaum AI, Lieber CS, Beattie DS, Rubin E. Characterization of shuttle mechanisms for the transport of reducing equivalents into mitochondria. Arch Biochem Biophys. 1973; 158:763–781. [PubMed: 4782532]
17. Kobayashi K, Sinasac DS, Iijima M, Boright AP, Begum L, Lee JR, Yasuda T, Ikeda S, Hirano R, Terazono H, Crackower MA, Kondo I, Tsui LC, Scherer SW, Saheki T. The gene mutated in adult-

onset type II citrullinaemia encodes a putative mitochondrial carrier protein. Nat Genet. 1999; 22:159–163. [PubMed: 10369257]

18. LaNoue KF, Williamson JR. Interrelationships between malate-aspartate shuttle and citric acid cycle in rat heart mitochondria. Metabolism. 1971; 20:119–140. [PubMed: 4322086]
19. Jomain-Baum M, Hanson RW. Regulation of hepatic gluconeogenesis in the guinea pig by fatty acids and ammonia. J Biol Chem. 1975; 250:8978–8985. [PubMed: 1194271]
20. Sugano T, Shiota M, Tanaka T, Miyamae Y, Shimada M, Oshino N. Intracellular redox state and stimulation of gluconeogenesis by glucagon and norepinephrine in the perfused rat liver. J Biochem. 1980; 87:153–166. [PubMed: 7358625]
21. Williamson JR, Scholz R, Browning ET. Control mechanisms of gluconeogenesis and ketogenesis. II. Interactions between fatty acid oxidation and the citric acid cycle in perfused rat liver. J Biol Chem. 1969; 244:4617–4627. [PubMed: 5808508]
22. Williamson JR, Scholz R, Browning ET, Thurman RG, Fukami MH. Metabolic effects of ethanol in perfused rat liver. J Biol Chem. 1969; 244:5044–5054. [PubMed: 4390471]
23. Perry RJ, CJ, Kursawe R, Titchenell PM, Zhang D, Perry CJ, Jurczak MJ, Abudukadier A, Han MS, Zhang XM, Ruan HB, Yang X, Caprio S, Kaech SM, Sul HS, Birnbaum MJ, Davis RJ, Cline GW, Petersen KF, Shulman GI. Hepatic acetyl CoA links adipose tissue inflammation to hepatic insulin resistance and type 2 diabetes. Cell. 2015; 160:745–758. [PubMed: 25662011]
24. Perry RJ, ZX, Zhang D, Kumashiro N, Camporez JP, Cline GW, Rothman DL, Shulman GI. Leptin reverses diabetes by suppression of the hypothalamic-pituitary-adrenal axis. Nat Med. 2014; 20:759–763. [PubMed: 24929951]
25. Sistare FD, Haynes RC Jr. The interaction between the cytosolic pyridine nucleotide redox potential and gluconeogenesis from lactate/pyruvate in isolated rat hepatocytes. Implications for investigations of hormone action. J Biol Chem. 1985; 260:12748–12753. [PubMed: 4044607]
26. Goodman LSLS, Brunton Laurence L, Chabner BruceKnollmann Björn C. 1906–2000 Goodman & Gilman's the pharmacological basis of therapeutics. 12. McGraw-Hill; 2011.
27. Duca FA, CC, Rasmussen BA, Zadeh-Tahmasebi M, Rutter GA, Filippi BM, Lam TK. Metformin activates a duodenal Ampk-dependent pathway to lower hepatic glucose production in rats. Nat Med. 2015; 21:506–511. [PubMed: 25849133]
28. Guigas B, BL, Taleux N, Foretz M, Wiernsperger N, Vertommen D, Andreelli F, Viollet B, Hue L. 5-Aminoimidazole-4-carboxamide-1-beta-D-ribofuranoside and metformin inhibit hepatic glucose phosphorylation by an AMP-activated protein kinase-independent effect on glucokinase translocation. Diabetes. 2006; 55:865–874. [PubMed: 16567505]
29. Zhou G, MR, Li Y, Chen Y, Shen X, Fenyk-Melody J, Wu M, Ventre J, Doebber T, Fujii N, Musi N, Hirshman MF, Goodyear LJ, Moller DE. Role of AMP-activated protein kinase in mechanism of metformin action. J Clin Invest. 2001; 108:1167–1174. [PubMed: 11602624]
30. Hundal RS, KM, Dufour S, Laurent D, Lebon V, Chandramouli V, Inzucchi SE, Schumann WC, Petersen KF, Landau BR, Shulman GI. Mechanism by which metformin reduces glucose production in type 2 diabetes. Diabetes. 2000; 49:2063–2069. [PubMed: 11118008]
31. Inzucchi S, MD, Spollett GR, Page SL, Rife FS, Walton V, Shulman GI. Efficacy and metabolic effects of metformin and troglitazone in type II diabetes mellitus. N Eng J Med. 1998; 338:867–872.
32. Chu CA, WN, Muscato N, Knauf M, Neal DW, Cherrington AD. The acute effect of metformin on glucose production in the conscious dog is primarily attributable to inhibition of glycogenolysis. Metabolism. 2000; 49:1619–1626. [PubMed: 11145127]
33. Mithieux G, GL, Bordet JC, Wiernsperger N. Intrahepatic mechanisms underlying the effect of metformin in decreasing basal glucose production in rats fed a high-fat diet. Diabetes. 2002; 51:139–143. [PubMed: 11756333]
34. Lavine JE, SJ, Van Natta ML, Molleston JP, Murray KF, Rosenthal P, Abrams SH, Scheimann AO, Sanyal AJ, Chalasani N, Tonascia J, Ünalp A, Clark JM, Brunt EM, Kleiner DE, Hoofnagle JH, Robuck PR. Nonalcoholic Steatohepatitis Clinical Research Network. Effect of vitamin E or metformin for treatment of nonalcoholic fatty liver disease in children and adolescents: the TONIC randomized controlled trial. JAMA. 2011; 305:1659–1668. [PubMed: 21521847]

35. Rakoski MO, SA, Rogers MA, Conjeevaram H. Meta-analysis: insulin sensitizers for the treatment of non-alcoholic steatohepatitis. Aliment Pharmacol Ther. 2010; 32:1211–1221. [PubMed: 20955440]
36. Shields WW, TK, Grice GA, Harrison SA, Coyle WJ. The Effect of Metformin and Standard Therapy versus Standard Therapy alone in Nondiabetic Patients with Insulin Resistance and Nonalcoholic Steatohepatitis (NASH): A Pilot Trial. Therap Adv Gastroenterol. 2009; 2:157–163.
37. Gormsen LC, SE, Christensen NL, Jakobsen S, Nielsen EHT, Munk OL, Tolbod LP, Jessen N, Nielsen S. Metformin does not affect postabsorptive hepatic free fatty acid uptake, oxidation or resecretion in humans: A 3-month placebo-controlled clinical trial in patients with type 2 diabetes and healthy controls. Diabetes Obes Metab. 2018 Epub ahead of print.
38. Ryle PR, CJ, Thomson AD. The effect of methylene blue on the hepatocellular redox state and liver lipid content during chronic ethanol feeding in the rat. Biochem J. 1985; 232:877–882. [PubMed: 4091827]
39. Baur JA, BM. Control of gluconeogenesis by metformin: does redox trump energy charge? Cell Metab. 2014; 20:197–199. [PubMed: 25100057]
40. He L, WF. Metformin action: concentrations matter. Cell Metab. 2015; 21:159–162. [PubMed: 25651170]
41. Puhakainen I, KV, Yki-Järvinen H. Lipolysis and gluconeogenesis from glycerol are increased in patients with noninsulin-dependent diabetes mellitus. J Clin Endocrinol Metab. 1992; 75:789–794. [PubMed: 1517368]
42. Nurjhan N, CA, Gerich J. Increased lipolysis and its consequences on gluconeogenesis in non-insulin-dependent diabetes mellitus. J Clin Invest. 1992; 89:169–175. [PubMed: 1729269]
43. Metformin alters the gut microbiome of individuals with treatment-naive type 2 diabetes, contributing to the therapeutic effects of the drug. Nature Medicine. 2017; 23:850–858.
44. Schlienger JL, FA, Marbach J, Freund H, Imler M. Effects of biguanides on the intermediate metabolism of glucose in normal and portal-strictured rats. Diabete Metab. 1979; 5:5–9. [PubMed: 446834]
45. Gormsen LC, SE, Jensen JB, Vendelbo MH, Jakobsen S, Munk OL, Hougaard Christensen MM, Brøsen K, Frøkiær J, Jessen N. In Vivo Imaging of Human 11C-Metformin in Peripheral Organs: Dosimetry, Biodistribution, and Kinetic Analyses. J Nucl Med. 2016; 57:1920–1926. [PubMed: 27469359]
46. Brønden AAA, Rohde U, Rehfeld JF, Holst JJ, Vilsbøll T, Knop FK. Single-dose Metformin Enhances Bile Acid-Induced GLP-1 Secretion in Patients with Type 2 Diabetes. Journal of Clinical Endocrinology & Metabolism. 2017 In press.
47. Timmins P, DS, Meeker J, Marathe P. Steady-state pharmacokinetics of a novel extended-release metformin formulation. Clin Pharmacokinet. 2005; 44:721–729. [PubMed: 15966755]
48. Larsen S, RR, Hansen CN, Madsbad S, Helge JW, Dela F. Metformin-treated patients with type 2 diabetes have normal mitochondrial complex I respiration. Diabetologia. 2012; 55:443–449. [PubMed: 22009334]
49. Said A, AA. Meta-Analysis of Randomized Controlled Trials of Pharmacologic Agents in Non-alcoholic Steatohepatitis. Ann Hepatol. 2017; 16:538–547. [PubMed: 28611274]
50. Sawangjit R, CB, Phisalprapa P, Saokaew S, Thakkinstian A, Kowdley KV, Chaiyakunapruk N. Comparative efficacy of interventions on nonalcoholic fatty liver disease (NAFLD): A PRISMA-compliant systematic review and network meta-analysis. Medicine (Baltimore). 2016; 95:e4529. [PubMed: 27512874]
51. Kim CW, AC, Kusunoki J, Anderson NN, Deja S, Fu X, Burgess SC, Li C, Ruddy M, Chakravarthy M, Previs S, Milstein S, Fitzgerald K, Kelley DE, Horton JD. Acetyl CoA Carboxylase Inhibition Reduces Hepatic Steatosis but Elevates Plasma Triglycerides in Mice and Humans: A Bedside to Bench Investigation. Cell Metab. 2017; 26:576. [PubMed: 28877461]
52. Konopka AR, ER, Robinson MM, Johnson ML, Carter RE, Schiavon M, Cobelli C, Wondisford FE, Lanza IR, Nair KS. Hyperglucagonemia Mitigates the Effect of Metformin on Glucose Production in Prediabetes. Cell Rep. 2016; 15:1394–1400. [PubMed: 27160898]

53. Lewis AJ, MJ, McCallum C, Rider OJ, Neubauer S, Heather LC, Tyler DJ. Assessment of Metformin-Induced Changes in Cardiac and Hepatic Redox State Using Hyperpolarized[1-13C]Pyruvate. Diabetes. 2016; 65:3544–3551. [PubMed: 27561726]
54. Qi H, NP, Schroeder M, Bertelsen LB, Palm F, Laustsen C. Acute renal metabolic effect of metformin assessed with hyperpolarised MRI in rats. Diabetologia. 2018; 61:445–454. [PubMed: 28936623]
55. Nattrass M, TP, Hinks L, Lloyd B, Alberti KGMM. Comparative effects of phenformin, metformin and glibenclamide on metabolic rhythms in maturity-onset diabetics. Diabetologia. 1977; 13:145–152. [PubMed: 404205]
56. Hussey EK, KA, O'Connor-Semmes R, Tao W, Rafferty B, Polli JW, James CD Jr, Dobbins RL. Safety, pharmacokinetics and pharmacodynamics of remogliflozin etabonate, a novel SGLT2 inhibitor, and metformin when co-administered in subjects with type 2 diabetes mellitus. BMC Pharmacol Toxicol. 2013; 14:25. [PubMed: 23631443]
57. Comte B, Vidal H, Laville M, Riou JP. Influence of thyroid hormones on gluconeogenesis from glycerol in rat hepatocytes: a dose-response study. Metabolism. 1990; 39:259–263. [PubMed: 2308516]
58. Gregory RB, Phillips JW, Berry MN. Reducing-equivalent transfer to the mitochondria during gluconeogenesis and ureogenesis in hepatocytes from rats of different thyroid status. Biochim Biophys Acta. 1992; 1137:34–38. [PubMed: 1356445]
59. Kneer N, Lardy H. Thyroid hormone and dehydroepiandrosterone permit gluconeogenic hormone responses in hepatocytes. Arch Biochem Biophys. 2000; 375:145–153. [PubMed: 10683260]
60. Drahota Z, PE, Endlicher R, Milerova M, Brejchova J, Vosahlikova M, Svoboda P, Kazdova L, Kalous M, Cervinkova Z, Cahova M. Biguanides inhibit complex I, II and IV of rat liver mitochondria and modify their functional properties. Physiol Res. 2014; 63:1–11. [PubMed: 24182344]
61. Reed MJ, MK, Entes LJ, Claypool MD, Pinkett JG, Brignetti D, Luo J, Khandwala A, Reaven GM. Effect of masoprocol on carbohydrate and lipid metabolism in a rat model of Type II diabetes. Diabetologia. 1999; 42:102–106. [PubMed: 10027587]
62. Perry RJ, PL, Cline GW, Butrico GM, Wang Y, Zhang X-M, Rothman DL, Petersen KF, Shulman GI. Non-Invasive Assessment of Hepatic Mitochondrial Metabolism by Positional Isotopomer NMR Tracer Analysis (PINTA). Nat Commun. 2017; 8:798. [PubMed: 28986525]
63. Perry RJ, KT, Zhang XM, Lee HY, Pesta D, Popov VB, Zhang D, Rahimi Y, Jurczak MJ, Cline GW, Spiegel DA, Shulman GI. Reversal of hypertriglyceridemia, fatty liver disease, and insulin resistance by a liver-targeted mitochondrial uncoupler. Cell Metab. 2013; 18:740–748. [PubMed: 24206666]
64. Alves TC, BD, Kibbey RG, Kahn M, Codella R, Carvalho RA, Falk Petersen K, Shulman GI. Regulation of hepatic fat and glucose oxidation in rats with lipid-induced hepatic insulin resistance. Hepatology. 2011; 53:1175–1181. [PubMed: 21400553]
65. Perry RJ, PL, Abulizi A, Kennedy L, Cline GW, Shulman GI. Mechanism for leptin's acute insulin-independent effect to reverse diabetic ketoacidosis. J Clin Invest. 2017; 127:657–669. [PubMed: 28112679]
66. Ayala JE, Samuel VT, Morton GJ, Obici S, Croniger CM, Shulman GI, WDH, McGuinness OP. Mouse Metabolic & Consortium NIH P C. Standard operating procedures for describing and performing metabolic tests of glucose homeostasis in mice. Dis Model Mech. 2010; 3:525–534. [PubMed: 20713647]
67. Passonneau JV, LV. A comparison of three methods of glycogen measurement in tissues. Anal Biochem. 1974; 60:405–412. [PubMed: 4844560]
68. Bligh EaDW. A rapid method of total lipid extraction and purification. Can J Biochem Physiol. 1959; 37:911–917. [PubMed: 13671378]

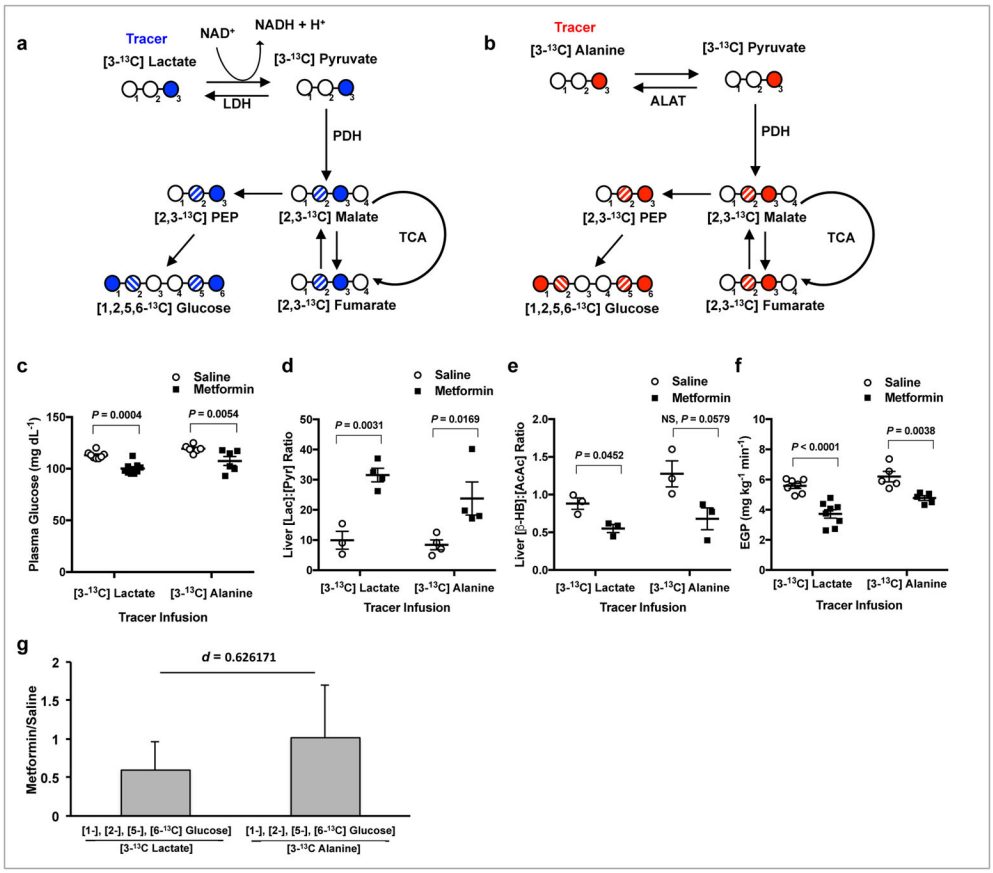

Figure 1.

Acute IV 50 mg kg^{-1} metformin treatment inhibits contributions from lactate but not alanine to hepatic gluconeogenesis in normal SD rats. (**a**) A schematic diagram illustrating that [3-^{13}C]lactate will enter gluconeogenesis via lactate dehydrogenase (LDH), regulated by the cytosolic redox state, and contribute to labeling in the 1 and 6 positions of glucose as well as the 2 and 5 positions due to isomerization during the conversion of fumarate to malate. PDH, pyruvate dehydrogenase; TCA, tricarboxylic acid; PEP, phosphoenolpyruvate. (**b**) A schematic diagram illustrating that [3-^{13}C]alanine is converted to pyruvate via alanine aminotransferase (ALAT) independent of redox state and will also label the 1,2,5, and 6 positions of glucose. (**c**) Plasma glucose levels in SD rats within 2 h after acute metformin or saline treatment and infused with either [3-^{13}C]lactate or [3-^{13}C]alanine tracer (**d**,**e**) The liver cytosolic redox state, as represented by the [lac]:[pyr] ratio, (**d**) and the liver mitochondrial redox state, as measured by the [β-OHB]:[AcAc] ratio, (**e**) in SD rats after acute metformin treatment and tracer infusion. (**f**) EGP of SD rats upon acute metformin treatment plus tracer infusion. (**g**) Contribution of lactate to glucose from [3-^{13}C]lactate and contribution of alanine to glucose from [3-^{13}C]alanine as determined by the ratio of label in the 1, 2, 5 and 6 positions of glucose in metformin-treated rat livers relative to saline-treated (metformin/saline) livers. Data are mean ± SEM (**a**–**f**) or mean ± SD (**g**), ([3-^{13}C]lactate, saline: $n = 8$, metformin: $n = 9$; [3-^{13}C]alanine, saline: $n = 6$, metformin: $n = 6$, biological replicates). For statistical analysis, P values were calculated by two-way *ANOVA* with

Sidak's multiple comparisons (**a**–**f**), and effect size *d* by Cohen's standard (**g**), and NS = not significant.

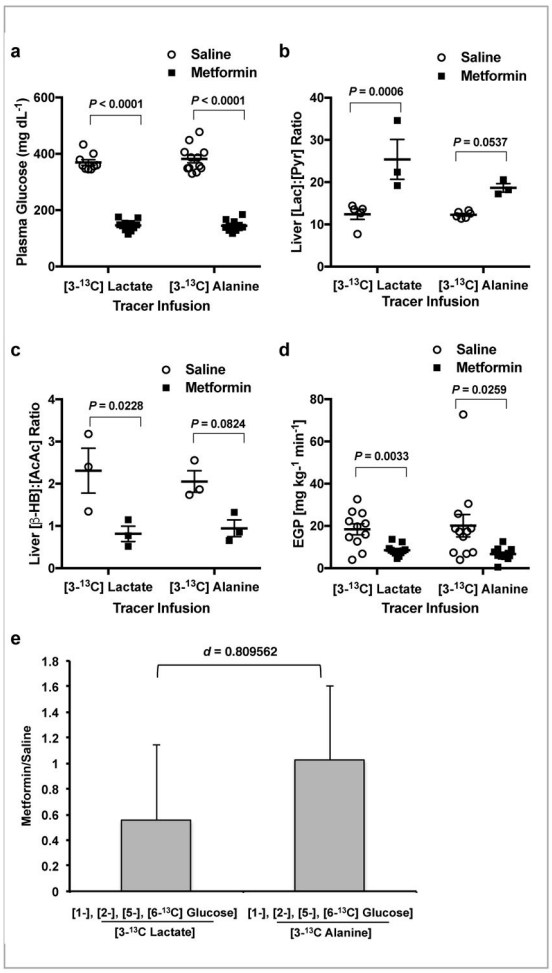

Figure 2.

Acute IV 50 mg kg^{-1} metformin treatment inhibits contributions from lactate but not alanine to hepatic gluconeogenesis in ZDF rats. (**a**) Fasting plasma glucose concentrations in ZDF rats acutely treated with metformin or saline over 2 h during [3-^{13}C]lactate and [3-^{13}C] alanine tracer infusions. (**b**) Liver [lac]:[pyr] ratio, a surrogate for the cytosolic redox state, and (**c**) liver [β-OHB]:[AcAc] ratio, representative of the mitochondrial redox state. (**d**) EGP rates in saline and metformin treated animals at 2 h post-treatment. (**e**) The contribution of lactate to glucose as determined by the metformin/saline ratio of the label in the 1, 2, 5 and 6 positions of glucose from [3-^{13}C] lactate. Contribution of alanine is indicated by the metformin/saline ratio of of the label in the 1, 2, 5 and 6 positions of glucose from [3-^{13}C]alanine. Data are mean ± SEM (**a–d**), or mean ± SD (**e**), ([3-^{13}C]lactate, saline: n=9, metformin: n=11; [3-^{13}C]alanine, saline: n=12, metformin: n=11, biological replicates). For statistical analysis, *P* values were calculated by two-way *ANOVA* with Sidak's multiple comparisons (**a–d**), and effect size *d* by Cohen's standard (**d**), and NS = not significant.

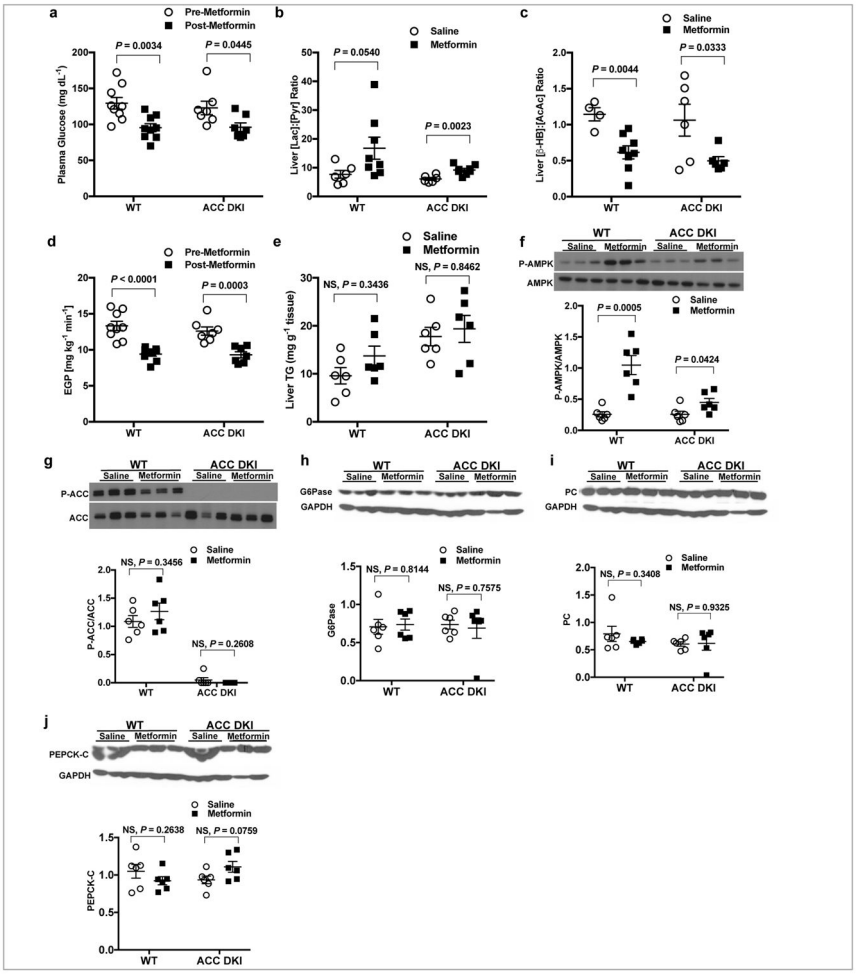

Figure 3.

Acute IV 50 mg kg^{-1} metformin treatment decreases fasting plasma glucose and inhibits EGP in the ACC DKI mouse model by modulating redox. (**a**) Fasting plasma glucose concentrations in the ACC DKI mice and WT littermates before and 2 h after acute metformin treatment. (**b**) Hepatic cytosolic redox state and (**c**) liver mitochondrial redox state in ACC DKI and WT mice 2 h post-metformin or saline treatment. (**d**) EGP 2 h post-metformin or saline treatment in WT and ACC DKI mice. (**e**) Hepatic triglyceride levels in WT and ACC DKI mice 2 h post-metformin or saline treatment. (**f**) Liver AMPK activation in WT and ACC DKI mice as determined by the ratio of phosphorylated AMPK (P-AMPK) to total AMPK protein. (**g**) Liver ACC activation as determined by the ratio of phosphorylated ACC (P-ACC) to total ACC protein in ACC DKI and the WT mice. Data are mean ± SEM (WT, n=7; ACC DKI, n=9 per group for plasma glucose (**a**), EGP (**d**); n=6 per group for liver redox (**b, c**), TG and protein expression (**e–g**). For statistical analysis, *P* values were calculated by two-way *ANOVA* with Sidak's multiple comparisons, and NS = not significant.

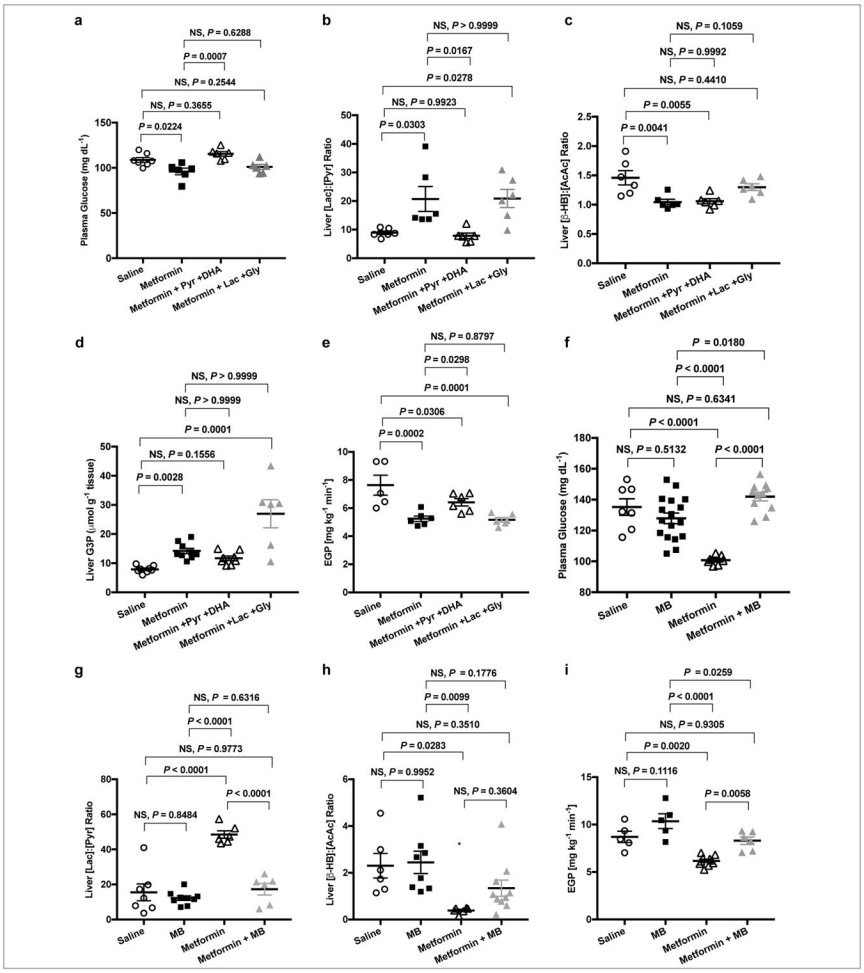

Figure 4.

Infusion of substrates (pyruvate and DHA), and infusion of methylene blue (MB), both abrogate the effects of acute IV 50 mg kg^{-1} metformin treatment on plasma glucose and EGP in normal SD rats. (**a**) Fasting plasma glucose concentrations in SD rats treated acutely with saline, metformin, or metformin combined with infusion of pyruvate and DHA (both substrates that do not alter cytosolic redox state when entering gluconeogenesis) or equimolar lactate and glycerol (both substrates that increase cytosolic redox state). (**b**) Liver [lac]:[pyr] ratio, (**c**) liver [β-OHB]:[AcAc] ratio, and (**d**) hepatic G-3-P concentrations 2 h following acute saline, metformin, metformin with pyruvate/DHA or metformin with lactate/glycerol treatment. (**e**) EGP at 2 h post-treatment. (**f**) Fasting plasma glucose with acute saline or metformin treatment with and without concomitant treatment with 2 mg/kg acute IV MB. (**g**) Effect of acute saline and metformin treatments with and without MB treatment on liver cytosolic redox state and (**h**) mitochondrial redox state. (**i**) EGP 2 h post-treatment. Data are mean ± SEM, (For substrate infusion (**a–e**): saline, n=7; metformin, n=6; pyruvate/DHA & metformin, n=6; pyruvate/DHA & metformin, n=6; biological replicates; for MB infusion (**f–i**): saline, n=8; MB, n=12; metformin, n=7; MB & metformin, n=10; biological replicates). For statistical analysis, *P* values were calculated by one-way *ANOVA* with Tukey's multiple comparisons test, and NS = not significant.

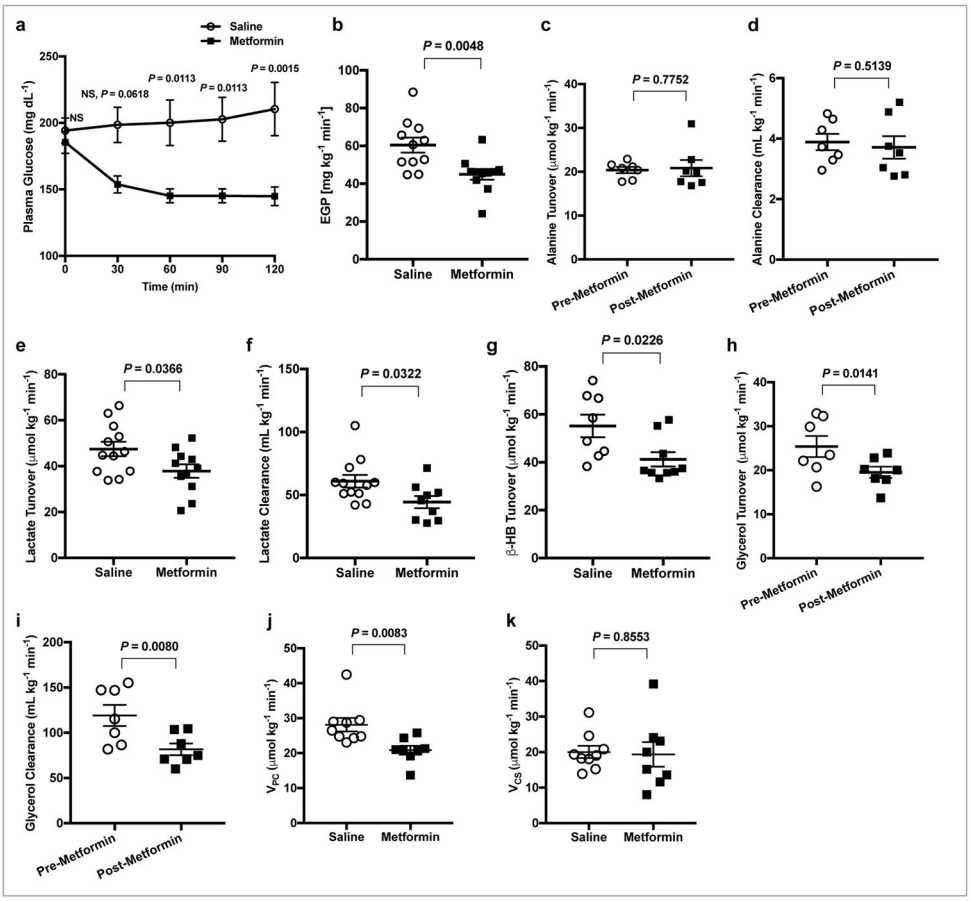

Figure 5.

Portal vein infusion of 50 mg kg^{-1} metformin acutely inhibits hepatic gluconeogenesis and selectively alters lactate, β-OHB and glycerol turnover and clearance rates without altering alanine turnover and alanine clearance rates or impacting mitochondrial citrate synthase flux (V_{CS}) in a HFD-STZ Sprague-Dawley rat model of type 2 diabetes (T2D). (**a**) Fasting plasma glucose concentrations in saline and metformin treated HFD-STZ rats over 2 h. (**b**) EGP rates in HFD-STZ rats 2 h post-metformin or saline treatment. (**c**) Alanine turnover and (**d**) clearance (clearance is mL of plasma cleared of substrate per minute) in before and after metformin treatment in HFD-STZ rats. (**e**) Lactate turnover, (**f**) lactate clearance and (**g**) β-OHB turnover rates in HFD-STZ rats treatment with metformin versus saline. (**h**) Glycerol turnover and (**i**) glycerol clearance rates before and after metformin treatment. (**j**) Liver pyruvate carboxylase flux (V_{PC}) and (**k**) hepatic mitochondrial citrate synthase flux (V_{CS}) in HFD-STZ rats post-metformin treatment versus saline. Data are mean ± SEM, (for **a**,**b**,**g**: saline, n=8, metformin n=9; for **e**: saline n=12, metformin n=11; for **f**: saline n=12, metformin n=9; for **c,d,h,i**: saline n=7, metformin n=7; for **j,k**: saline n=8, metformin n=8 biological replicates). For statistical analysis, *P* values were calculated by two-tailed unpaired Student's *t*-test (**a,b,e-g,j,k**) and two-tailed paired Student's *t*-test (**c,d,h,i**), and NS = Not significant.

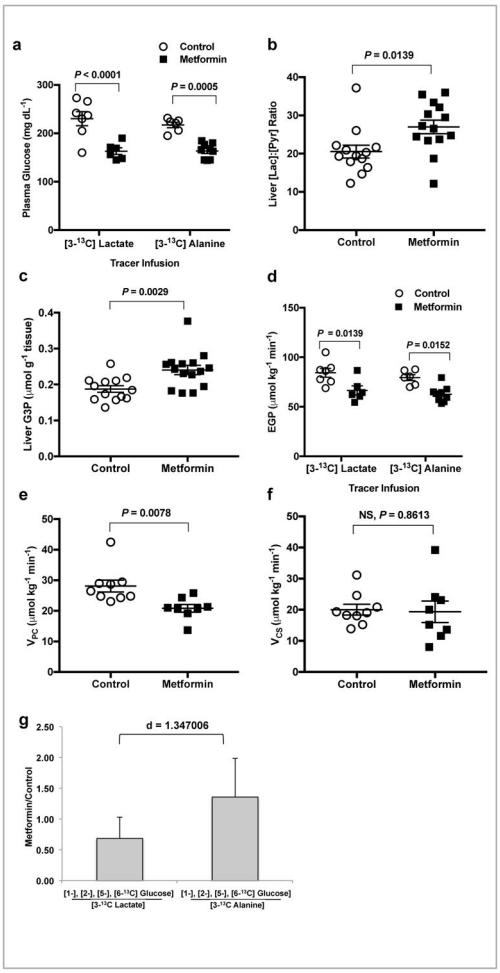

Figure 6.

Chronic oral metformin treatment (3.5 mg ml^{-1} in the drinking water for 14 days) specifically inhibits contributions from lactate but not alanine to hepatic gluconeogenesis without impacting mitochondrial citrate synthase flux (V_{CS}) in a HFD-STZ Sprague-Dawley rat model of T2D. (**a**) Fasting plasma glucose concentrations in chronic oral metformin treated rats from both [3-^{13}C]lactate and [3-^{13}C]alanine tracer infusion cohorts. (**b**) Hepatic cytosolic redox state as determined by the [lac]:[pyr] ratio. (**c**) Liver G-3-P concentrations in chronically treated metformin or saline rats post tracer infusion. (**d**) EGP rates in rats from both the [3-^{13}C]lactate and [3-^{13}C]alanine tracer infusion cohorts. (**e**) Liver pyruvate carboxylase flux (V_{PC}) and (**f**) hepatic mitochondrial citrate synthase flux (V_{CS}). (**g**) Contribution of lactate to glucose indicated by the metformin/saline ratio of glucose labeled in the 1, 2, 5 and 6 positions from [3-^{13}C] lactate. Contribution of alanine is indicated by the metformin/saline ratio of labeling in the 1, 2, 5 and 6 positions of glucose from [3-^{13}C] alanine. Data are mean ± SEM (**a–f**) or mean ± SD (**g**). (For **a**,**d**,**g**: [3-^{13}C]lactate, saline: n=7, metformin: n=6; [3-^{13}C]alanine, saline: n=6, metformin: n=9,; for **b**,**c**: saline: n=13, metformin: n=15; for **e**,**f**: saline: n=9, metformin: n=8 biological replicates). For statistical analysis, *P* values were calculated by two-way ANOVA (**a,d**), unpaired two-tailed *t*-test with

Welch's correction (**a**–**c,e,f**) and effect size *d* by Cohen's standard (**g**) and NS = not significant.